

# Optimal Rational Circles of Degrees Five and Six

Helmut E. Bez<sup>1</sup>, Thomas J. Wetzel<sup>2</sup>

<sup>1</sup> *Department of Computer Science, Loughborough University  
Loughborough, Leicestershire, LE11 3TU, UK  
email: h.e.bez@lboro.ac.uk*

<sup>2</sup> *Wetzel Associates, Inc.  
4022 E. Greenway Rd., Ste. 11 PMB 189, Phoenix, AZ 85032-4760, USA  
email: TJWetzel@CompuServe.com*

**Abstract.** This paper presents new low degree, complete Bézier circles with positive weights. Specifically: two symmetric, quintic parametrizations — optimized towards arc-length parametrization in  $L^2$  and  $L^\infty$  norms — are developed and a new degree six circle with a symmetric, near arc-length parametrization is presented. Properties of the parametrizations are discussed and compared.

*Key Words:* Rational paths, circle parametrization, optimization

*MSC 2000:* 68U05, 53A04

## 1. Introduction

Parametrization of the circle remains an active research topic for applications in computer graphics and computer aided geometric design [5]. Techniques for the construction of B-spline circles have been reviewed in [7]. Single segment Bézier circles have been considered in [3, 8, 9, 10]; CHOU [3] makes the case for single segment solutions and shows that positive weight circles are minimally of degree five. The material presented in this paper complements the literature on full Bézier circles by considering the ‘rate-of-tracing’ of rational parametrizations; i.e., the relative density of evaluated points on the circle for equal increments of the parameter. Only parametrizations proportional to the arc-length parametrization have exactly constant rate-of-tracing; however, no such rational parametrizations of the circle exist. This follows either from general known results on rational parametrization [4] or from the fact, which can be demonstrated by elementary means, that the only solutions to the system of functional equations

$$f^2(t) + g^2(t) = 1, \quad f'^2(t) + g'^2(t) = 1$$

are the harmonic functions  $f(t) = \cos(t + \alpha)$ ,  $g(t) = \sin(t + \alpha)$ , where  $\alpha$  is any constant; hence there is essentially only one arc-length parametrization of the circle and it is not rational.

Nevertheless rational parametrizations with near-constant rate-of-tracing can be constructed and are of interest for a number of reasons, including: the visual quality of an arc drawn at a given incremental resolution and the efficient conversion of parametrized shapes into CNC instructions. A documented series of rational exact circles [8] is known to approach arc-length parametrization as the degree of the representation increases [2]. However high-precision to arc-length is not achieved until the degree is excessively high — of order at least  $O(10^2)$ .

In this paper new exact rational circles of degrees 5 and 6 are constructed with parametrizations optimized towards the arc-length parametrization. The computation combines an inductive process for the construction of rational parametrizations — as described by the authors in [2] — with a novel process to optimize the parametrizations towards near-constant rate-of-tracing'. In each case, the rate-of-tracing function is a sum of 'harmonic' components — each corresponding to a term in the inductive construction. Explicit vertex and weight data for the circles is provided, and may be applied directly by practitioners without reference to the means of construction.

## 2. Paths

If  $I$  is an interval of  $\mathbb{R}$ , then a regular planar *path* is a  $C^1$  function  $p: I \rightarrow \mathbb{R}^2$  with  $p' \neq 0$ . The set of paths on  $I$  is denoted  $\mathcal{P}_I$ . A *curve* is an equivalence class of paths, written  $[p]$  where  $p \in \mathcal{P}_{I_p}$ , for some  $I_p$ , and  $q \sim p$  if and only if  $q = p \circ \phi$  for some  $C^1$  invertible function  $\phi: I_q \rightarrow I_p$ . Equivalent paths have the same graph. A curve  $[p]$  is said to be *rational* if there exists a  $q \in [p]$  where  $q = (q_x, q_y)$  is such that  $q_x$  and  $q_y$  are rational. In this case there exists a function  $\phi$  such that  $p \circ \phi$  is rational; such functions, applied in this paper to complete circles, are of the form  $\phi: [0, 1] \rightarrow [0, 2\pi]$ . The set  $\mathcal{P}_I$  is a vector space over  $\mathbb{R}$  under the usual scalar multiplication and addition operations. In addition a binary operator  $*$  can be defined on  $\mathcal{P}_I$  by complex multiplication; i.e.,

$$p * q = (p_x q_x - p_y q_y, p_x q_y + p_y q_x)$$

where  $p = (p_x, p_y)$  and  $q = (q_x, q_y)$ .

## 3. Circle parametrization

### 3.1. Measures of distance between parametrizations

The  $L^2$ -norm  $\|\cdot\|_2$  is the natural generalization of Euclidean length, it is widely used in approximation theory and used in this paper to measure the distance between exact rational parametrizations of the circle and the arc-length parametrization in an optimization process. The value  $\|f - g\|_2$  is an 'average' measure of the difference between  $f$  and  $g$ ; the maximum difference is measured by the  $L^\infty$ -norm and this is used in the paper as an alternative means of evaluating the  $L^2$ -optimized parametrizations of the circles constructed.

If  $f$  is as above and  $f_{ap}$  is an approximation of  $f$ , then the relative error in the approximation with respect to a norm  $\|\cdot\|$  is

$$\frac{\|f - f_{ap}\|}{\|f\|}.$$

The unit circle centred at  $(0,0)$  is denoted  $S^1$  and, in the remainder of the paper,  $p = (p_x, p_y)$  denotes the arc-length parametrization of  $S^1$ ; i.e.,

$$p(\theta) = (\cos \theta, \sin \theta) \text{ for } 0 \leq \theta \leq 2\pi.$$

Let  $c = (c_x, c_y)$  be a parametrization of  $S^1$  on the interval  $[0, 1]$  and let  $\phi_c$  denote the polar angle at  $t \in [0, 1]$ . Clearly  $c_x(t) = \cos \phi_c(t)$ ,  $c_y(t) = \sin \phi_c(t)$ ,  $\phi_c = \tan^{-1}(c_y/c_x)$  and

$$c = (\cos \phi_c, \sin \phi_c) = p \circ \phi_c$$

where  $p$  denotes the arc-length parametrization  $p(\theta) = (\cos \theta, \sin \theta)$ .

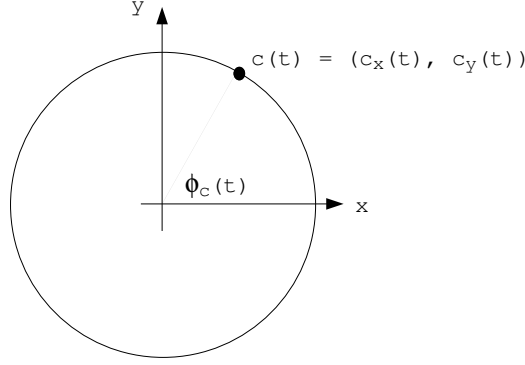


Figure 1: Parametrization of  $S^1$

Let  $c_1 = (c_{1,x}, c_{1,y})$  and  $c_2 = (c_{2,x}, c_{2,y})$  be any two parametrizations of  $S^1$  subtending  $2\pi$  on  $[0, 1]$ . We have, for  $i \in \{1, 2\}$

$$\phi_{c_i} = \tan^{-1} \left( \frac{c_{i,y}}{c_{i,x}} \right), \quad \phi'_{c_i} = c_{i,x} c'_{i,y} - c'_{i,x} c_{i,y}$$

where  $\phi_{c_i}: [0, 1] \rightarrow [0, 2\pi]$ , with  $\phi_{c_i}(0) = 0$  and  $\phi_{c_i}(1) = 2\pi$ ,  $\phi'_{c_i}: [0, 1] \rightarrow \mathbb{R}$  and  $c_i = p \circ \phi_i$ . A number of  $L^2$ -norms may be used to measure ‘distance’ between parametrizations  $c_1$  and  $c_2$ ; including

$$\|c_1 - c_2\|_2 = \left[ \int_0^1 |c_1(t) - c_2(t)|^2 dt \right]^{\frac{1}{2}}$$

and

$$\|\phi'_{c_1} - \phi'_{c_2}\|_2 = \left[ \int_0^1 |\phi'_{c_1}(t) - \phi'_{c_2}(t)|^2 dt \right]^{\frac{1}{2}}.$$

The first is a measure of the average difference between the arc lengths traced by  $c_1$  and  $c_2$  and  $\|\phi'_{c_1} - \phi'_{c_2}\|_2$  measures the average difference between the rate of arc length tracing of  $c_1$  and  $c_2$ .

It is traditional in computer aided geometric design to define rational paths on the interval  $[0, 1]$ ; however to measure the ‘closeness’ a rational parametrization of  $S^1$  to the arc-length parametrization it is necessary to compare it, using a suitable norm, with  $p(\theta) = (\cos \theta, \sin \theta)$  — which is defined on  $[0, 2\pi]$ . Hence for the purposes of comparison a common interval of definition is required and the re-scaled arc-length parametrization  $p^*(t) = (\cos 2\pi t, \sin 2\pi t)$ ;  $0 \leq t \leq 1$  is therefore used. If  $\gamma: [0, 1] \rightarrow [0, 2\pi]$  is defined by  $\gamma(t) = 2\pi t$  then  $p^* = p \circ \gamma$ , and  $p^*$  is such that  $\phi_{p^*}(t) = 2\pi t$ .

The construction of the near arc-length parametrized circles described in the paper uses an optimization procedure that minimizes the  $L^2$  difference between the rates of tracing of the near arc-length candidate path with the exact path  $p^*$ . Hence for the purposes of the

optimization process, the distance between  $p^*$  and a candidate parametrization  $c$  is measured as

$$\|\phi'_c - \phi'_{p^*}\|_2 = \left[ \int_0^1 |\phi'_c(t) - 2\pi|^2 dt \right]^{\frac{1}{2}}.$$

The optimal solutions, obtained in this way, can be evaluated in other norms; for example  $\|c - p^*\|_2$  is a measure of the average chordal separation of  $p^*$  and  $c$ . For all parametrizations  $c_1$  and  $c_2$  of  $S^1$  on  $[0, 1]$  we have:

$$\|c_1 - c_2\|_2 = \left[ \int_0^1 |c_1(t) - c_2(t)|^2 dt \right]^{\frac{1}{2}} = \sqrt{2} \left[ \int_0^1 (1 - c_1(t) \cdot c_2(t))^2 dt \right]^{\frac{1}{2}},$$

and

$$\|c_1 - c_2\|_2 \leq \|c_1 - c_2\|_\infty.$$

### 3.2. Symmetric parametrizations of the circle

**Definition 1.** A parametrization  $c = p \circ \phi_c$  of the circle is said to be symmetric if

$$\phi_c(t) + \phi_c(1 - t) = 2\pi \quad \text{for all } t \in [0, 1].$$

Equivalently we could define  $c$  to be symmetric (i) if  $\phi'_c(1 - t) = \phi'_c(t)$ , i.e., if the graph of the rate-of-tracing function  $\phi'_c: [0, 1] \rightarrow \mathbb{R}$  is symmetric about the point  $t = \frac{1}{2}$ , or (ii) if

$$(p \circ \phi_c)(t) = R(p \circ \phi_c)(1 - t)$$

where  $R$  is the reflection matrix  $\begin{bmatrix} 1 & 0 \\ 0 & -1 \end{bmatrix}$ .

All symmetric parametrizations are such that  $\phi_c(\frac{1}{2}) = \pi$ . Only symmetric parametrizations of the circle are considered in this paper. The reasons for this include:

- the parametrization being approximated — i.e., the exact arc-length parametrization — is symmetric;
- existing rational parametrizations against which those constructed in the paper are measured, i.e., the standard series [8] and the CHOU quintic, are all symmetric;
- the objective functions, for the optimization process, have fewer variables for symmetric constructions.

### 3.3. Product parametrizations

If  $c_1$  and  $c_2$  are the parametrizations of  $S^1$  defined above then, assuming  $c_1$  subtends an angle of  $\Delta_1$  and  $c_2$  subtends an angle  $\Delta_2$ , the product  $c_1 * c_2$  determines a parametrization of  $S^1$  that subtends  $\Delta_1 + \Delta_2$ . It follows that  $\phi_{c_1 * c_2} = \phi_{c_1} + \phi_{c_2}$  and that the rate-of-tracing function for  $c_1 * c_2$  is  $\phi'_{c_1 * c_2} = \phi'_{c_1} + \phi'_{c_2}$ . This generalizes to a product of  $n$  terms for which the angle subtended is  $\sum_{i=1}^n \Delta_i$  and for which  $\phi'_{c_1 * \dots * c_n} = \sum_{i=1}^n \phi'_{c_i}$ .

### 3.4. Induced parametrizations

If  $q: I \rightarrow \mathbb{R}^2$  is a path in the plane we can define  $\pi(q)$  as the formal quotient  $\pi(q) = q/|q|$ . If  $q$  is suitably regular then  $\pi(q)$  determines a parametrization of the circle on  $I$ . Similarly the product parametrization

$$\pi(q^2) = \frac{q * q}{|q * q|}$$

and, more generally,  $\pi(q^k)$ , for  $k \in \mathbb{N}$ , determine parametrizations of the circle. We call  $\pi(q^k)$  parametrizations of the circle ‘induced’ by the ‘primitive’ (or ‘source’) path  $q$ . If  $q = (u, v)$  then  $\pi(q^2)$  has the component form

$$\pi(q^2) = \frac{1}{u^2 + v^2} (u^2 - v^2, 2uv);$$

more generally we define, for paths  $q_1, \dots, q_n$ , the product parametrizations

$$\pi_n(q_1, \dots, q_n) = \frac{q_1 * \dots * q_n}{|q_1 * \dots * q_n|}$$

and  $\pi_n(q_1^k, \dots, q_n^k)$ . With suitable regularity conditions these also determine parametrizations of the circle — referred to in this paper as parametrizations induced on the circle by the ‘primitive’ paths  $q_1, \dots, q_n$ . Product parametrizations of the form  $\pi_n(q_1^2, \dots, q_n^2)$ , where the paths  $q_1, \dots, q_n$  are polynomial of degree 1, are rational and paths of this form are fundamental to the work of this paper. We note that if  $q_1 = (u_1, v_1)$  and  $q_2 = (u_2, v_2)$  then the induced parametrization  $\pi_2(q_1^2, q_2^2)$  of the circle is such that  $\pi_2(q_1^2, q_2^2) = \pi(q_3^2)$ , where  $q_3$  is given by  $q_3 = (u_1, v_1) * (u_2, v_2)$ . The product parametrization  $c_1 * c_2$  may be written as  $\pi_2(c_1, c_2)$ .

## 4. Induced rational parametrizations of the circle

### 4.1. Rational parametrization of the circle

If  $q = (u, v)$  where  $u$  and  $v$  are polynomial functions, then the induced parametrization

$$\pi(q^2) = \frac{1}{u^2 + v^2} (u^2 - v^2, 2uv)$$

is rational. It follows from KUBOTA’s theorem [6] that all rational parametrizations of the circle are of the form  $\pi(q^2)$  where  $q = (u, v)$  and  $u$  and  $v$  are polynomial functions. From the fundamental theorem of algebra we have  $q = q_1 * \dots * q_n$ , for some degree one polynomial functions  $q_1, \dots, q_n$ ; hence

$$\pi(q^2) = \pi((q_1 * \dots * q_n)^2) = \pi_n(q_1^2, \dots, q_n^2).$$

It is therefore true that:

- every rational parametrization of the circle may be written as an induced parametrization  $\pi_n(q_1^2, \dots, q_n^2)$ , where  $q_1, \dots, q_n$  are degree one primitives.

### 4.2. Quadratic parametrizations of circular arcs induced by a single degree-one primitive

We define, for  $\lambda > 0$  and  $0 < \Delta < \pi/2$ , a degree-one primitive  $F_{\lambda, \Delta}$  on  $[0, 1]$  by

$$F_{\lambda, \Delta}(t) = (1 - t)(1, 0) + t\lambda(\cos \Delta, \sin \Delta),$$

as  $\lambda \neq 0$  it follows that  $|F_{\lambda, \Delta}|(t) \neq 0$  for all  $t$  and  $\pi(F_{\lambda, \Delta}^2) = \frac{F_{\lambda, \Delta} * F_{\lambda, \Delta}}{|F_{\lambda, \Delta}|^2}$  is a well-defined induced parametrization of the circle; it subtends  $0 < 2\Delta < \pi$  on  $[0, 1]$  and has the explicit form

$$\pi(F_{\lambda, \Delta}^2)(t) = \frac{(1, 0)(1 - t)^2 + 2\lambda \cos \Delta(1, \tan \Delta)(1 - t)t + \lambda^2(\cos 2\Delta, \sin 2\Delta)t^2}{(1 - t)^2 + \lambda(\cos \Delta)2t(1 - t) + \lambda^2 t^2}.$$

Writing  $F_{\lambda,\Delta} = (u_{\lambda,\Delta}, v_{\lambda,\Delta})$  we have

$$\tan \frac{\phi_{\lambda,\Delta}}{2}(t) = \frac{v_{\lambda,\Delta}}{u_{\lambda,\Delta}} = \frac{t \lambda \sin \Delta}{(1-t) + t \lambda \cos \Delta}$$

from which we obtain

$$\phi'_{\lambda,\Delta}(t) = \frac{2\lambda \sin \Delta}{|F_{\lambda,\Delta}|^2(t)}.$$

The near arc-length Bézier circles described later in the paper are induced from quadratic primitives of the form  $F_{\lambda,\Delta}$  — with strong reference to the properties of their rate-of-tracing functions  $\phi'_{\lambda,\Delta}$  discussed below.

### 4.3. Properties of the rate-of-tracing function $\phi'_{\lambda,\Delta}$

**Proposition 1.** *The function  $\phi'_{\lambda,\Delta}$  is strictly positive with a single (maximum) turning point at  $t = T(\lambda, \Delta)$  where*

$$T(\lambda, \Delta) = \frac{1 - \lambda \cos \Delta}{1 - 2\lambda \cos \Delta + \lambda^2}.$$

*The graph of  $\phi'_{\lambda,\Delta}$  is symmetric about the point  $t = T(\lambda, \Delta)$  and  $\phi'_{\lambda,\Delta}$  tends to zero as  $t \rightarrow \pm\infty$ .*

*Proof.* This is immediate from the following: as  $\lambda > 0$  the quadratic  $|F_{\lambda,\Delta}|^2$  is (i) strictly positive, (ii) tends to infinity as  $t \rightarrow \pm\infty$  and (iii) has a single positive minimum value, which occurs at  $t = T(\lambda, \Delta)$  where

$$T(\lambda, \Delta) = \frac{1 - \lambda \cos \Delta}{1 - 2\lambda \cos \Delta + \lambda^2}. \quad \square$$

Fig. 2(a) illustrates the general shape of the graph of  $\phi'_{\lambda,\Delta}$ , as quantified in Proposition 1.

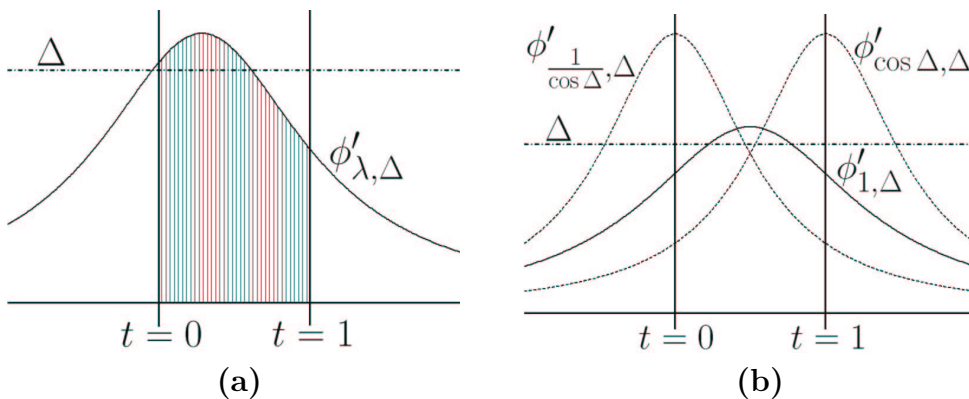


Figure 2: (a) The function  $\phi'_{\lambda,\Delta}$

(b) Special cases of  $\phi'_{\lambda,\Delta}$

**Corollary 1.** *For all  $0 < \Delta < \frac{\pi}{2}$ :*

$$T\left(\frac{1}{\cos \Delta}, \Delta\right) = 0, \quad T(1, \Delta) = \frac{1}{2} \quad \text{and} \quad T(\cos \Delta, \Delta) = 1.$$

Corollary 1 identifies the position of the turning point of  $\phi'_{\lambda,\Delta}$  for three significant values of  $\lambda$ ; i.e., for  $\lambda = 1$  the turning point is at the mid-point  $t = \frac{1}{2}$  of the interval of parametrization  $[0, 1]$ , for  $\lambda = \cos \Delta$ ,  $\phi'_{\lambda,\Delta}$  turns at  $t = 1$  and for  $\lambda = 1/\cos \Delta$  it turns at  $t = 0$ . Fig. 2(b) shows graphs of  $\phi'_{\lambda,\Delta}$  for these values of  $\lambda$ .

Corollary 2, below, shows how the turning point position varies continuously along the  $t$ -axis with respect to values of  $\lambda \in (0, \infty)$  and, in particular, the symmetric relationship between the graphs of  $\phi'_{\lambda,\Delta}$  and  $\phi'_{\lambda^{-1},\Delta}$ . This symmetry property is exploited in the construction of the near arc-length parametrized circles presented later in the paper.

**Corollary 2.** *It can be shown that:*

- if  $0 < \lambda < \cos \Delta$  then  $T(\lambda, \Delta) > 1$
- if  $\cos \Delta \leq \lambda \leq 1/\cos \Delta$  then  $0 \leq T(\lambda, \Delta) \leq 1$
- if  $1/\cos \Delta < \lambda < \infty$  then  $T(\lambda, \Delta) < 0$ ,
- and the ‘symmetry’ property  $T(\lambda^{-1}, \Delta) = 1 - T(\lambda, \Delta)$ .

It follows from the symmetry property that the graphs of  $\phi'_{\lambda,\Delta}$  and  $\phi'_{\lambda^{-1},\Delta}$  are reflections each of the other in the line  $t = \frac{1}{2}$  — as shown in Fig. 3(b). Fig. 3(a) shows graphs of  $\phi'_{\lambda,\pi/4}$  for values of  $\lambda$  in each of the sub-intervals  $I_+ = (0, \cos \Delta)$ ,  $I = (\cos \Delta, 1/\cos \Delta)$  and  $I_- = (1/\cos \Delta, \infty)$  of  $(0, \infty)$ .

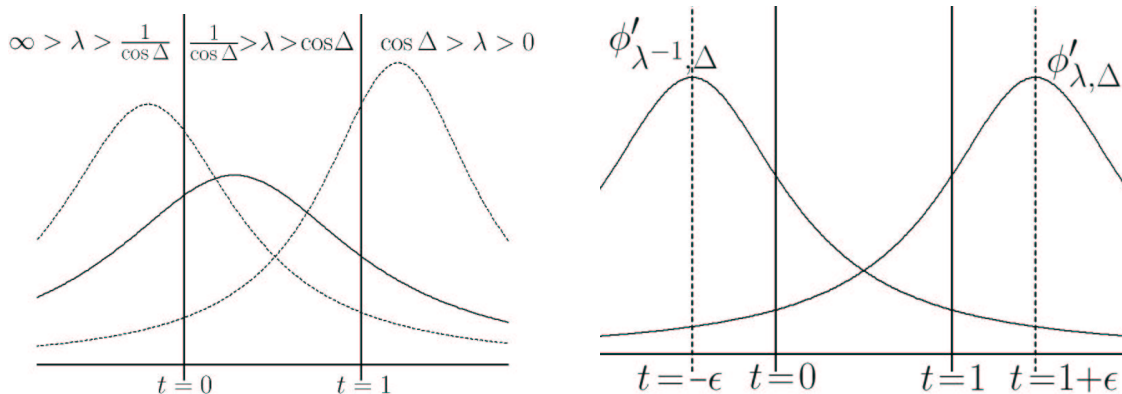


Figure 3: (a) Graphs of  $\phi'_{\lambda,\Delta}$  for  $\lambda$  in each of the intervals  $I_+$ ,  $I$  and  $I_-$   
 (b) The symmetry property of  $\phi'_{\lambda,\Delta}$

#### 4.4. Product parametrizations of circular arcs induced by multiple primitives

A single primitive may be used to induce a rational parametrization of  $S^1$ . However, as will be illustrated later, these parametrizations have strongly ‘bell’ shaped rate-of-tracing functions; similar to that shown in Fig. 5(b). Such induced parametrizations of  $S^1$  are not therefore near-arc-length.

To illustrate how the use of distinct primitives can produce symmetric, near-constant rate-of-tracing functions on  $[0, 1]$ , consider the degree-one primitives  $F_{\lambda_1,\Delta}$  and  $F_{\lambda_2,\Delta}$  and the associated induced parametrization

$$c_{\lambda_1,\lambda_2} = \pi(F_{\lambda_1,\Delta}^2, F_{\lambda_2,\Delta}^2).$$

This parametrization subtends a circular arc of  $4\Delta$  on the interval  $[0, 1]$  and has the rate-of-tracing function

$$\phi'_{\lambda_1, \lambda_2, \Delta} = \phi'_{\lambda_1, \Delta} + \phi'_{\lambda_2, \Delta}.$$

It follows from the symmetry property of  $T(\lambda, \Delta)$  — see Corollary 2 — that graphs of sums of the form  $\phi'_{\lambda, \lambda^{-1}, \Delta} = \phi'_{\lambda, \Delta} + \phi'_{\lambda^{-1}, \Delta}$  are symmetric about the point  $t = \frac{1}{2}$ . In fact, for a suitably chosen value of  $\lambda^*$ , of  $\lambda$ , we can achieve

$$\phi'_{\lambda^*, \lambda^{*-1}, \Delta} = \phi'_{\lambda^*, \Delta} + \phi'_{\lambda^{*-1}, \Delta} \approx 4\Delta \text{ on } [0, 1];$$

the rational parametrization corresponding to this ‘optimum’ value of  $\lambda$  therefore has near-arc-length rate-of-tracing.

By definition  $\lambda > 0$ , however it follows from Corollary 1 that  $\lambda^* \neq 1$  — because at this value both of the components of the rate-of-tracing function have maxima at  $t = \frac{1}{2}$  and cannot therefore yield near-constant rate-of-tracing on  $[0, 1]$ . In fact for  $\Delta = \pi/4$  the optimum value is  $\lambda^* \approx 1.5586278$  and a near-arc-length parametrized semi-circle is obtained. Fig. 4 shows graphs of an optimized rate-of-tracing function and its two components, for a typical value of  $\Delta$  in the range  $0 < \Delta \leq \pi/4$ .

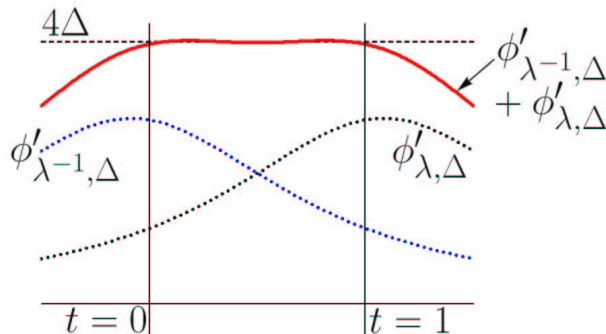


Figure 4: A ‘near constant’ function on  $[0, 1]$  as a sum  $\phi'_{\lambda, \Delta} + \phi'_{\lambda^{-1}, \Delta}$  of the ‘harmonic components’  $\phi'_{\lambda, \Delta}$  and  $\phi'_{\lambda^{-1}, \Delta}$

To parametrize a full circle on  $[0, 1]$  requires that  $\Delta = \pi/2$ . With such a large values of  $\Delta$  it is not possible to achieve a near-constant rate-of-tracing of the quality illustrated in Fig. 4 using just two primitives. Fig. 10 is more typical of the best that can be achieved for a full circle with two primitives. Hence for  $\Delta$  in the range  $\pi/4 < \Delta \leq \pi/2$ , induced parametrizations using three, or more, primitives should be used if near-arc-length rate-of-tracing is required.

The above is a special case of the following more general strategy for the construction of low degree near arc-length parametrizations of the circle subtending a designated angle  $\theta$  on  $[0, 1]$ : i.e.,

- induce a parametrization  $\pi_k(F_{\lambda_1, \Delta_1}^2, \dots, F_{\lambda_k, \Delta_k}^2)$  of the circle using a sequence,  $F_{\lambda_i, \Delta_i}$ ,  $0 \leq i \leq k$ , of degree-one primitives

where the  $\lambda_i$  and  $\Delta_i$  are chosen in such a way that:

- $2 \sum_{i=1}^k \Delta_i = \theta$
- the sum  $\phi'_{\lambda_1, \Delta_1} + \dots + \phi'_{\lambda_k, \Delta_k}$  of the rate-of-tracing functions of the quadratics  $F_{\lambda_k, \Delta_k}^2$  is symmetrical about the point  $t = \frac{1}{2}$  and

$$\phi'_{\lambda_1, \Delta_1} + \dots + \phi'_{\lambda_k, \Delta_k} \approx 2(\Delta_1 + \dots + \Delta_k) \text{ on } [0, 1].$$



#### 4.5. Documented rational circles as induced parametrizations

CHOU's quartic circle, [3], may be expressed as the induced parametrization

$$c_4 = \pi_2(F_{1,\pi/2}^2, F_{1,\pi/2}^2);$$

it has a zero weight coefficient in rational Bézier form. However if the degree elevated by one, the quintic path  $c_5$ , so constructed, has all positive weights.

The series of even degree rational parametrizations of  $S^1$ , described in [8], is such that the parametrization of degree  $2n$  may be expressed as the induced parametrization

$$c_{2n} = \pi(F_{1,\pi/n}^{2n}).$$

#### 4.6. Quartic and quintic Bézier circles

For any  $\lambda > 0$ , an induced, rational, symmetric quartic parametrization of  $S^1$  may be defined by

$$c_{4,\lambda} = \pi_2(F_{\lambda,\pi/2}^2, F_{\lambda^{-1},\pi/2}^2) = \frac{F_{\lambda,\pi/2}^2 * F_{\lambda^{-1},\pi/2}^2}{|F_{\lambda,\pi/2}^2|^2 |F_{\lambda^{-1},\pi/2}^2|^2}$$

from which the weights of  $c_{4,\lambda}$  may be computed as:

$$w_{0,4} = 1; \quad w_{1,4} = 0; \quad w_{2,4} = \frac{1}{6} \left( \lambda^2 + \frac{1}{\lambda^2} \right); \quad w_{3,4} = 0; \quad w_{4,4} = 1.$$

If the degree of  $c_{4,\lambda}$  is raised by one to a quintic, denoted  $c_{5,\lambda}$ , then the weights of  $c_{5,\lambda}$  are all positive and are given explicitly (see Appendix 1) by:

$$w_{0,5} = 1; \quad w_{1,5} = \frac{1}{5}; \quad w_{2,5} = \frac{1}{10} \left( \lambda^2 + \frac{1}{\lambda^2} \right); \quad w_{3,5} = \frac{1}{10} \left( \lambda^2 + \frac{1}{\lambda^2} \right); \quad w_{4,5} = \frac{1}{5}; \quad w_{5,5} = 1.$$

We can write, in terms of the quartic Bézier basis  $\{b_{i,4}\}$ ,

$$c_{4,\lambda} = \frac{b_{0,4}(1,0) + \frac{1}{2}(\lambda + \lambda^{-1})b_{1,4}(0,1) + \frac{1}{6}(4 + \lambda^2 + \frac{1}{\lambda^2})b_{2,4}(-1,0) + \frac{1}{2}(\lambda + \lambda^{-1})b_{3,4}(0,-1) + b_{4,4}(1,0)}{b_{0,4} + w_{2,4}b_{2,4} + b_{4,4}}$$

and in terms of the quintic Bézier basis  $\{b_{i,5}\}$  we have

$$c_{5,\lambda} = \frac{b_{0,5}(1,0) + b_{1,5}(\frac{1}{5}, \frac{4A}{5}) + b_{2,5}(-\frac{3C}{5}, \frac{2A}{5}) + b_{3,5}(-\frac{3C}{5}, -\frac{2A}{5}) + b_{4,5}(\frac{1}{5}, -\frac{4A}{5}) + b_{5,5}(1,0)}{b_{0,5} + w_{1,5}b_{1,5} + w_{2,5}b_{2,5} + w_{3,5}b_{3,5} + w_{4,5}b_{4,4} + b_{5,5}}$$

where

$$A = \frac{1}{2}(\lambda + \lambda^{-1}); \quad B = \frac{1}{10} \left( \lambda^2 + \frac{1}{\lambda^2} \right); \quad C = \frac{1}{6} \left( 4 + \lambda^2 + \frac{1}{\lambda^2} \right).$$

Incorporating the weights into the numerator gives

$$c_{5,\lambda} = \frac{b_{0,5}(1,0) + \frac{1}{5}b_{1,5}(1,4A) + Bb_{2,5}(-\frac{3C}{5B}, \frac{2A}{5B}) + Bb_{3,5}(-\frac{3C}{5B}, -\frac{2A}{5B}) + \frac{1}{5}b_{4,5}(1,-4A) + b_{5,5}(1,0)}{b_{0,5} + \frac{1}{5}b_{1,5} + Bb_{2,5} + Bb_{3,5} + \frac{1}{5}b_{4,4} + b_{5,5}}$$

from which the vertices of  $c_{5,\lambda}$  can be identified as

$$v_0 = (1,0); \quad v_1 = (1,4A); \quad v_2 = \left( -\frac{3C}{5B}, \frac{2A}{5B} \right); \quad v_3 = \left( -\frac{3C}{5B}, -\frac{2A}{5B} \right); \quad v_4 = (1,-4A); \quad v_5 = (1,0).$$

The parametrizations  $c_{4,\lambda}$  and  $c_{5,\lambda}$  have the same rate-of-tracing function, namely:

$$\phi'_\lambda = \phi_{\lambda,\pi/2} + \phi'_{\lambda^{-1},\pi/2}.$$

The surface

$$\zeta_4(\lambda, t) = \phi'_\lambda(t) - 2\pi,$$

which is shown in Fig. 5(a), represents the deviation of the rate-of-tracing function from  $2\pi$  on the interval  $0 \leq t \leq 1$  over a range of  $\lambda$  values; the  $t$ -axis runs left-to-right with  $\lambda$  running front-to-back and  $\zeta$  on the vertical axis. CHOU's circle corresponds to the section at  $\lambda = 1$ , i.e., the strongly 'bell shaped' curve on the front edge of the surface and shown in Fig. 5(b); the curve is the sum of two identical harmonic components — also shown in 5(b).

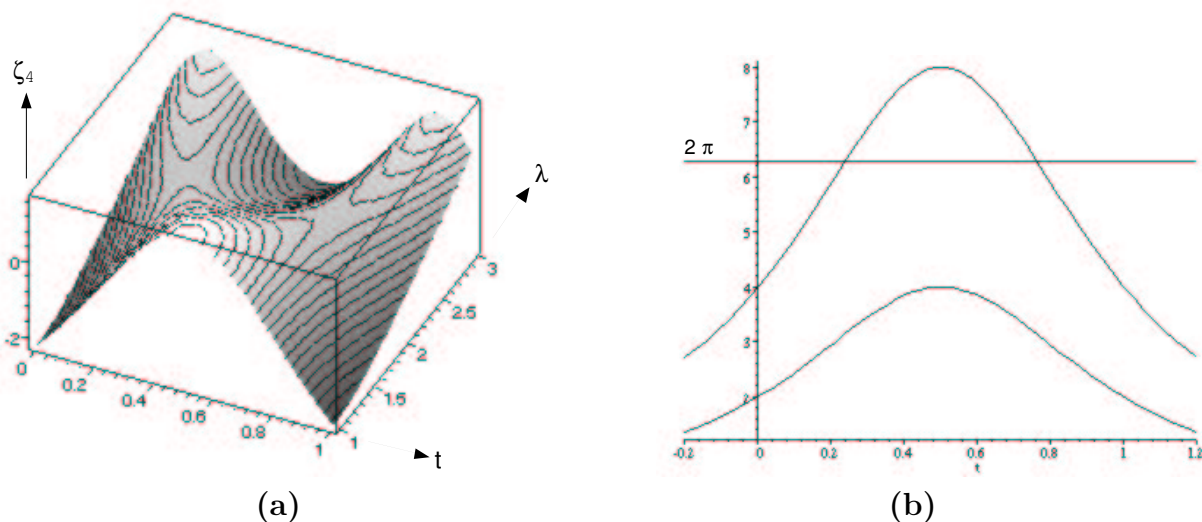


Figure 5: (a) The surface  $\zeta_4$ .  
(b) The 'bell' shaped rate-of-tracing function  $\phi'_5$  of the CHOU path  $c_5$ .

#### 4.7. The $L^\infty$ -optimized quintic circle

Fig. 6 shows the  $(\lambda, \zeta)$ -projection of  $\zeta_4$ , from which it can be seen that the maximum deviation from arc-length (i.e., the 'thickness' of the surface  $\zeta_4$ ) is least near the point  $\lambda = 2.4$ . This 'special' value of  $\lambda$  therefore minimizes the  $L^\infty$  distance

$$\mu_{4,\infty}(\lambda) = \|\phi'_{\lambda,\pi/2} + \phi'_{\lambda^{-1},\pi/2} - 2\pi\|_\infty = \sup_{[0,1]} |\phi'_{\lambda,\pi/2} + \phi'_{\lambda^{-1},\pi/2} - 2\pi|.$$

An  $L^\infty$ -optimized circle,  $c_{5,\infty}$ , may therefore be determined as follows;

- find the  $\lambda$  value,  $\lambda^*$ , that minimizes  $\mu_{4,\infty}$ ,
- determine the quartic  $c_{4,\infty}$  corresponding to  $\lambda^*$ ,
- elevate the degree of  $c_{4,\infty}$  by one to determine the quintic  $c_{5,\infty}$ .

The value of  $\lambda^*$  may be computed to be  $\lambda = 1 + \sqrt{2}$ ; this is also the value that corresponds to the 'symmetry' condition

$$\phi'_\lambda(0) = \phi'_\lambda(1/2) = \phi'_\lambda(1)$$

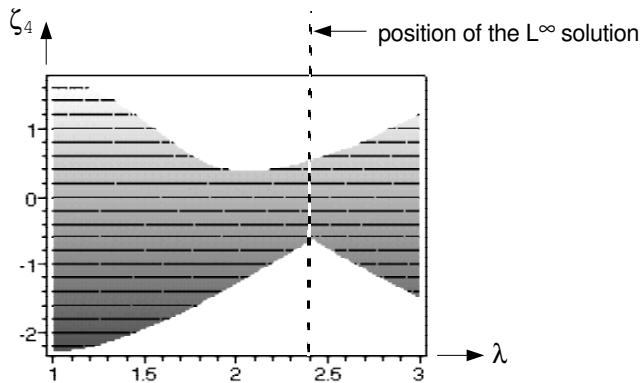


Figure 6: The  $(\lambda, \zeta)$ -projection of  $\zeta_4$  — showing the position of the  $L^\infty$  solution

for  $\phi'_\lambda$ . We denote the rate-of-tracing function of the optimized quintic circle by  $\phi'_{5,\infty}$ . For  $c_{5,\infty}$ , we have

$$\mu_{4,\infty}(1 + \sqrt{2}) = 0.6263306 \quad \text{and} \quad \|c_{5,\infty} - p^*\|_2 = 0.043869$$

which should be compared with

$$\mu_{4,\infty}(1) = 2.2831854 \quad \text{and} \quad \|c_5 - p^*\|_2 = 0.203269$$

for  $c_5$ . The graph of  $\phi'_{5,\infty}$  is shown in Fig. 7.

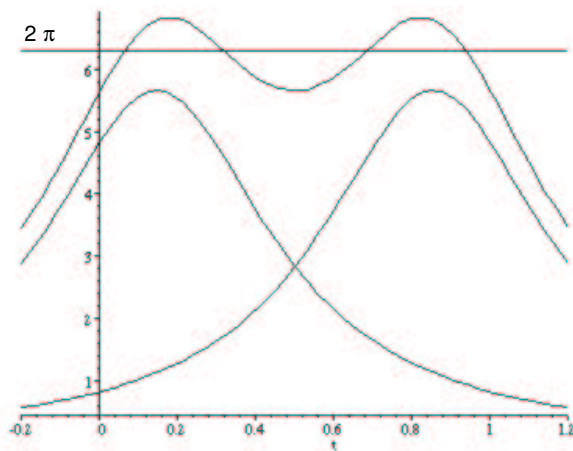


Figure 7: The graphs of rate-of-tracing function  $\phi'_{5,\infty}$  and its two components for the circle  $c_{5,\infty}$

Fig. 8 compares the rate-of-tracing of both CHOU’s path, 8(a), and the  $L^\infty$ -optimized circle, 8(b), with the arc-length parametrized path; in this figure hollow circles represent the arc-length parametrization and filled black circles show the rational parametrizations. Fig. 9 compares the control polygon of the CHOU circle with that of  $c_{5,\infty}$ .

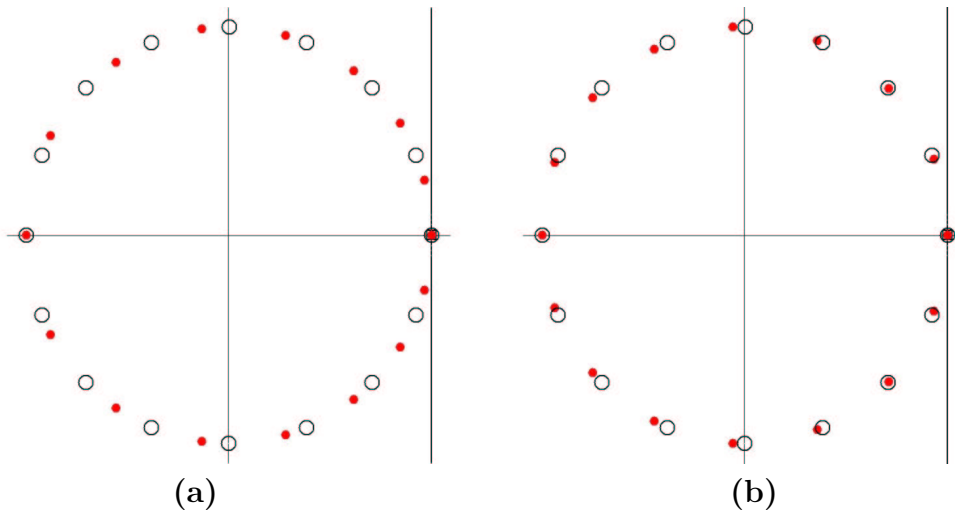


Figure 8: Comparison of **(a)** the CHOU circle  $c_5$  and **(b)** the optimized circle  $c_{5,\infty}$  with the arc-length parametrized circle  $p^*$

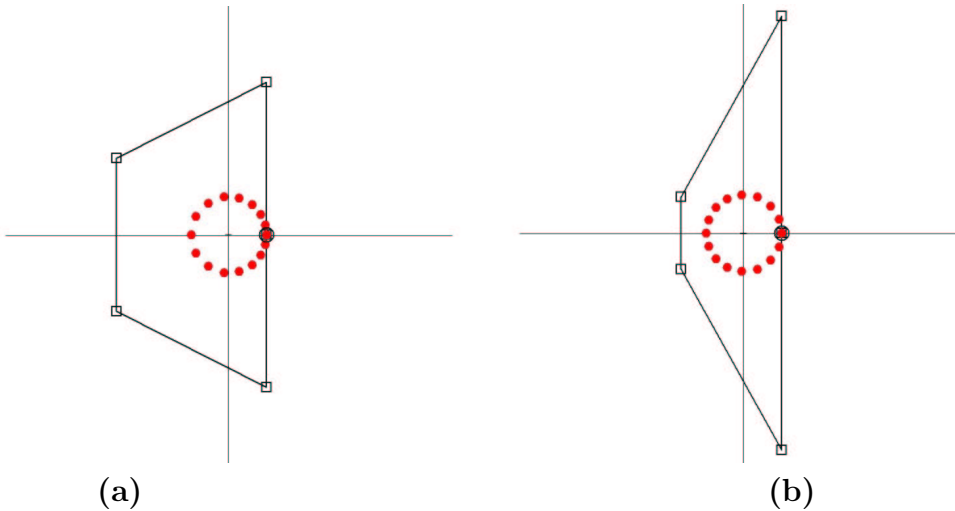


Figure 9: Bézier polygons for **(a)** the CHOU circle  $c_5$  and **(b)**  $L^\infty$ -optimized circle  $c_{5,\infty}$

#### 4.8. The $L^2$ -optimized quintic circle

An ' $L^2$ -optimized', symmetric, quintic parametrization, having all positive weights and denoted  $c_{5,2}$ , may now be constructed as follows:

- find the value,  $\lambda^*$ , of  $\lambda$  that minimizes the integral

$$\mu_{4,2}(\lambda) = \int_0^1 |\phi'_{\lambda, \pi/2}(t) + \phi'_{\lambda^{-1}, \pi/2}(t) - 2\pi|^2 dt,$$

- determine the quartic,  $c_{4,2}$ , corresponding to  $\lambda^*$ ,
- elevate the degree of  $c_{4,2}$  to obtain the  $L^2$ -optimized quintic parametrization  $c_{5,2}$ .

The minimum of  $\mu_{4,2}$  occurs at  $\lambda^* \approx 2.23065$ , we have

$$\mu_{4,2}(2.23065) = 0.33117 \quad \text{and} \quad \|c_{5,2} - p^*\|_2 = 0.0245263$$

which should be compared with the values

$$\mu_{4,2}(1) = 1.2862 \quad \text{and} \quad \|c_5 - p^*\|_2 = 0.203269$$

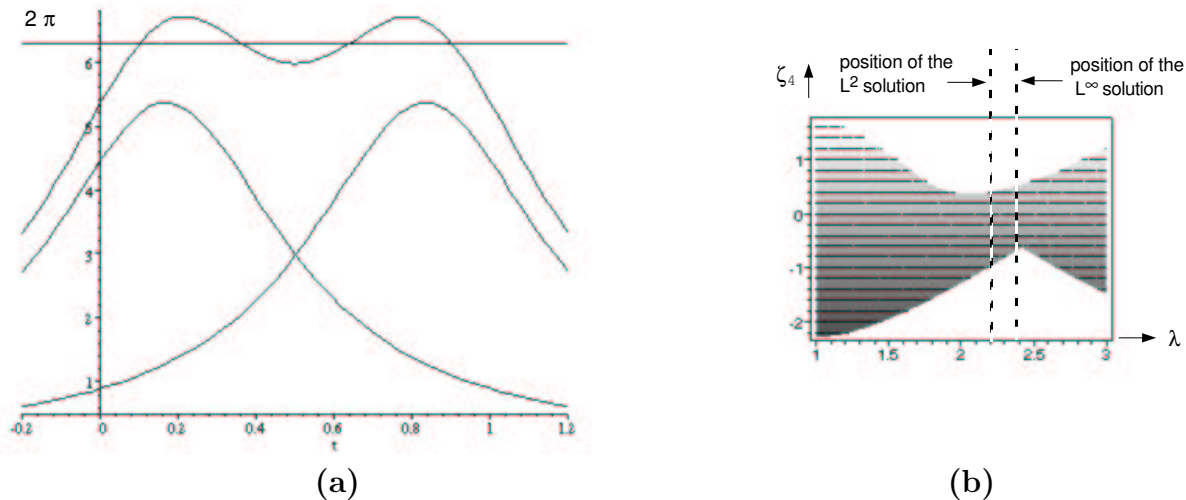


Figure 10: **(a)** The graphs of  $\phi'_{5,2}$  and its two components for the  $L^2$ -optimized circle  $c_{5,2}$   
**(b)** The  $(\lambda, \zeta)$ -projection of  $\zeta_4$  — showing the positions of the  $L^2$  and  $L^\infty$  solutions

for the CHOU parametrization. The rate-of-tracing function  $\phi'_{5,2}$ , and its harmonic components, for the  $L^2$ -optimized circle  $c_{5,2}$  is shown in Fig. 10(a) — the greatest deviation from  $2\pi$  occurs at the boundary points  $t = 0$  and  $t = 1$  of the parametric domain  $[0, 1]$  of the circle. Fig. 10(b) shows the relative positions of the  $L^2$  and  $L^\infty$  solutions.

Although the paths  $c_{5,2}$  and  $c_{5,\infty}$  are significantly closer to arc-length parametrization than the CHOU path  $c_5$ , it is shown below that much better results can be obtained by inducing parametrizations of  $S^1$  from 3 primitives.

#### 4.9. An $L^2$ -optimized, induced degree six rational circle

In this section a degree 6, positive weight, near arc-length, symmetric, rational parametrization of the complete circle is induced from three primitives.

The general properties of the rate-of-tracing functions discussed earlier suggest that to ensure:

- the symmetry of the rate-of-tracing function of the induced parametrization about  $t = \frac{1}{2}$ ,
- and that  $2\pi$  is subtended on the interval  $[0, 1]$

requires the selection of primitives of the form  $F_{\lambda,\Delta}$ ,  $F_{\lambda^{-1},\Delta}$  and  $F_{1,\pi-2\Delta}$ , and application of the construction

$$\pi_3(F_{\lambda,\Delta}^2, F_{1,\pi-2\Delta}^2, F_{\lambda^{-1},\Delta}^2)$$

for some values of  $\lambda$  and  $\Delta$ .

An optimization computation to minimize the distance

$$\mu(\lambda, \Delta) = \|\phi'_{\lambda,\Delta} + \phi'_{1,\pi-2\Delta} + \phi'_{\lambda^{-1},\Delta} - 2\pi\|_2$$

between  $\pi_3(F_{\lambda,\Delta}^2, F_{1,\pi-2\Delta}^2, F_{\lambda^{-1},\Delta}^2)$  and the arc length path, yields a minimum of

$$\mu_6 \approx 0.82369 \times 10^{-2}$$

at

$$\Delta \approx \Delta^* = 0.291\pi, \text{ and } \lambda \approx \lambda^* = 2.2915.$$

The  $L^2$ -optimized degree 6 parametrization  $c_6 = \pi_3(F_{\lambda^*, \Delta^*}^2, F_{1, \pi-2\Delta^*}^2, F_{\lambda^{*-1}, \Delta^*}^2)$  has a relative  $L^2$  approximation error to arc-length of less than 0.14% and is closer to arc-length than the degree 60 parametrization  $\pi(F_{\pi/30}^{60})$  of the series  $\pi(F_{1, \pi/n}^{2n})$  described in [8]. The  $L^2$  positional separation can be calculated as

$$\|c_6 - p^*\|_2 = 0.436762 \times 10^{-3}.$$

Clearly  $\pi(F_{1, \pi/6}^6)$  corresponds to the choices  $\Delta = \frac{\pi}{3}$  and  $\lambda = 1$  in  $\pi_3(F_{\lambda, \Delta}^2, F_{1, \pi-2\Delta}^2, F_{\lambda^{-1}, \Delta}^2)$ . Fig. 11 shows the  $L^2$ -optimized parametrization. The parametrization  $c_6$  can be expressed

$$c_6 = p \circ \varphi_6$$

where  $p$  is the arc-length parametrization and

$$\varphi_6 = \phi_{\lambda^*, \Delta^*} + \phi_{1, \pi-2\Delta^*} + \phi_{\lambda^{*-1}, \Delta^*}.$$

The weights and vertices of  $c_6$  are given in the Appendix to the paper.

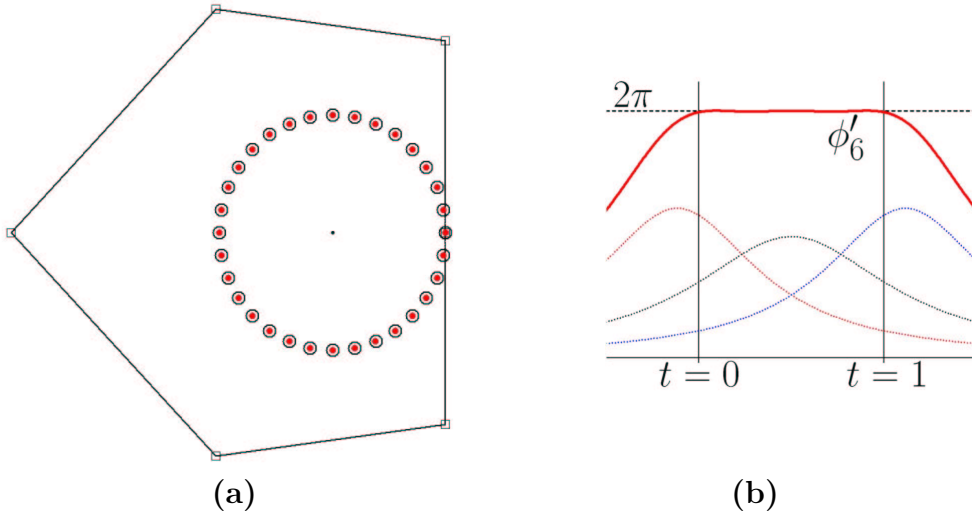


Figure 11: (a) The graph of  $c_6$  (b)  $\phi'_6$  and its three components

Near arc-length rational parametrizations of  $S^1$  of degrees 8, 10, 12, ... may be constructed using similar methods. Unlike the quintic case, for degrees  $\geq 6$  there is little point in considering optimal solutions in norms other than  $L^2$  — this is due to the extreme flatness of the  $\zeta$  surfaces near the  $L^2$  solution, from which it follows that the optimal  $L^\infty$  solution is necessarily very close to the optimal  $L^2$  solution. The situation is depicted in Fig. 12 for  $c_6$ , where the function  $\zeta_6$  and its  $(\lambda, \zeta)$ -projection are shown. For  $\zeta_6$  it can be seen that there is a section near  $\lambda = 2.2915$  where the surface exhibits almost no deviation from  $2\pi$  on the interval  $0 \leq t \leq 1$ ; hence the  $L^2$ - and  $L^\infty$ -optimized solutions for circles of degree  $\geq 6$  are virtually indistinguishable.

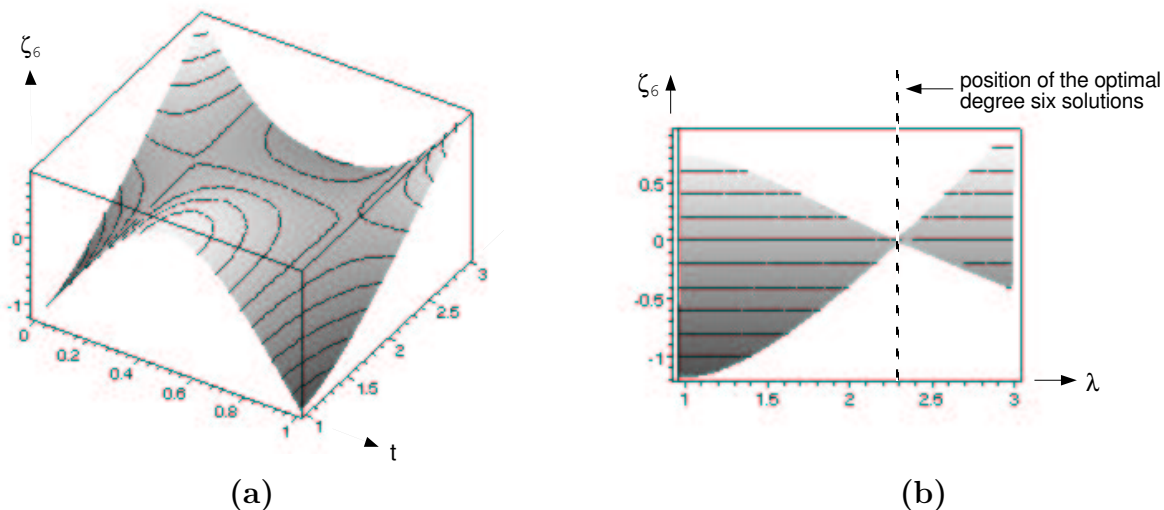


Figure 12: (a) The surface  $\zeta_6$  for degree 6 induced parametrizations  
 (b) Projection of  $\zeta_6$  onto the  $(\lambda, \zeta)$  plane

### Appendix — weights and vertices of the optimal circles

The weight and vertex data,  $w_i, v_i$ , for the  $L^2$ -optimized quintic circle  $c_{5,2}$  — corresponding to  $\lambda = 2.23065$  — are:

$i$	$w_i$	$v_i$
0	1	( 1.000000000, 0.000000000)
1	1/5	( 1.000000000, 5.357899644)
2	0.5176772153	(-1.772682258, 1.034988500)
3	0.5176772153	(-1.772682258, -1.034988500)
4	1/5	( 1.000000000, -5.357899644)
5	1	( 1.000000000, 0.000000000)

The data for the quintic  $L^\infty$ -optimized circle  $c_{5,\infty}$ , corresponding to  $\lambda = 1 + \sqrt{2}$ , given exactly and to eight decimal places for comparison with the data for  $c_{5,2}$ , are:

$i$	$w_i$	$v_i$
0	1	(1, 0) = ( 1.000000000, 0.000000000)
1	1/5	(1, $4\sqrt{2}$ ) = ( 1.000000000, 5.656854249)
2	3/5	( $-5/3$ , $2\sqrt{2}/3$ ) = (-1.666666667, 0.942809042)
3	3/5	( $-5/3$ , $-2\sqrt{2}/3$ ) = (-1.666666667, -0.942809042)
4	1/5	(1, $-4\sqrt{2}$ ) = ( 1.000000000, -5.656854249)
5	1	(1, 0) = ( 1.000000000, 0.000000000)

The data for the near-arc-length degree six circle  $c_6$  are:

$i$	$w_i$	$v_i$
0	1.00000000	( 1.00000000, 0.00000000)
1	0.63997907	( 1.00000000, 1.62906557)
2	0.64192096	(-1.03192823, 1.89695176)
3	0.50963710	(-2.83901798, 0.00000000)
4	0.64192096	(-1.03192823, -1.89695176)
5	0.63997907	( 1.00000000, -1.62906557)
6	1.00000000	( 1.00000000, 0.00000000)

## References

- [1] H.E. BEZ, T.J. WETZEL: *Constructive Path Algebra — a tool for design, parametrization and visualisation*. Proc. Eurographics UK 2002, IEEE Computer Society Press, 97–104.
- [2] H.E. BEZ, T.J. WETZEL: *Induced rational parametrizations of special curves*. International Journal of Computer Mathematics **80**, 1093–1109 (2003).
- [3] J.J. CHOU: *Higher order Bézier circles*. Computer-Aided Design **27**, 303–309 (1995).
- [4] R.T. FAROUKI, T. SAKKALIS: *Real rational curves are not ‘unit speed’*. Comput. Aided Geom. Design **8**, 151–157 (1991).
- [5] A. ARDESHIR GOSHTASBY: *Parametric circles and spheres*. Computer-Aided Design **35**, 487–494 (2003).
- [6] K.K. KUBOTA: *Pythagorean triples in unique factorization domains*. Amer. Math. Monthly **79**, 503–505 (1972).
- [7] L. PIEGL, W. TILLER: *A menagerie of rational B-spline circles*. IEEE Computer Graphics and Applications **21**, 48–56 (1989).
- [8] J. SÁNCHEZ-REYES: *Higher order Bézier circles*. Computer-Aided Design **29**, 469–472 (1997).
- [9] J. SÁNCHEZ-REYES: *Harmonic rational Bézier curves, p-Bézier curves and trigonometric polynomials*. Comput. Aided Geom. Design **15**, 909–923 (1998).
- [10] J. SÁNCHEZ-REYES: *Bézier representation of epitrochoids and hypotrochoids*. Computer-Aided Design **31**, 747–750 (1999).

Received January 14, 2004; final form June 23, 2004